Normal vibrational analysis of a rigid rod polymer: poly(*p*-phenylene terephthalamide)

P. K. Kim, C. Chang and S. L. Hsu*
Department of Polymer Science and Engineering, University of Massachusetts, Amherst, Massachusetts 01003, USA
(Received 4 February 1985)

The authors have analysed the vibrational spectra of poly(*p*-phenylene terephthalalamide). The structure used is identical to that obtained from X-ray diffraction and all the internal coordinates have been defined. A specific set of non-redundant symmetry coordinates was used in the normal vibrational calculation. Satisfactory assignments were made in the region above 800 cm^{-1}. The authors have estimated the ultimate tensile modulus using diagonal force constants and the dispersion curves associated with PPTA. The modulus value was obtained from the slope of the longitudinal acoustic vibration near the zone centre. A value of 241 GPa was obtained.

(Keywords: normal vibrational analysis; poly(*p*-phenylene terephthalamide) rigid rod polymers; tensile modulus; force constants; dispersion curves)

INTRODUCTION

The attractive mechanical properties such as high modulus and strength of poly(*p*-phenylene terephthalate) (PPTA),

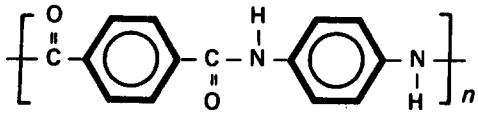

are due to the inherent stiff chain structure and the extremely highly ordered structure introduced by processing from the liquid crystalline or the anisotropic state[1]. However, the entire processing procedure is rather complex and the final solid state morphology or structure can be altered by varying intermediate steps. Because these differences in structure may be correlated to the deformation mechanisms present and ultimately to the mechanical properties achievable[2,3], detailed studies of different morphological units at various size levels are greatly needed.

The unit cell of PPTA has been known for some time[4,5]. Furthermore, traditional scattering techniques such as X-ray or electron diffraction and various microscopy studies have shown that the solid structure of the fibres may be complicated. The existence of extreme morphological heterogeneity such as skin-core or chain orientation differences have been revealed[6-8]. However, the details of conformational or chain packing differences resulting either from variations in processing procedures or in post-processing treatments remain to be investigated.

In our laboratory, we have used vibrational spectroscopy as the primary method to study microstructures of rigid rod polymers such as PPTA. Unlike the efforts being expended to study the structures of other polymers, there has been only limited quantitative spectroscopic studies of these rigid chain polymers[2,3,9-14]. Even though the experimental difficulties involved in working with these polymers are considerable, structural information obtained with the vibrational spectroscopic technique is supplementary and complementary to the results obtained from earlier characterization studies. Information regarding chain conformation and packing is most commonly sought after by the use of vibrational spectroscopy. This is true when bands are well assigned, and especially when transition dipole angles are known. There are also a number of experimental and theoretical analyses using vibrational spectroscopy estimating stress-induced changes in polymers[9,12,15-19]. However, the quantitative analysis of these rigid chain polymers is seldom carried out because of their complex structures and extremely low molecular symmetry, which makes their complicated infra-red and Raman spectra difficult to analyse.

Even after overcoming the experimental problems associated with working with strong acids as solvents, the high temperatures needed, small fibre diameter, etc., theoretical vibrational spectroscopic analysis remains as a considerable challenge. For complex molecules such as PPTA, a considerable number of branching and cyclic redundancies exist. Usually, in order to preserve the local symmetry of a molecule, the internal coordinates containing these redundancies are used in the normal vibrational analysis. The number of force constants necessarily then increases, causing them to be nearly meaningless when transferred from one molecule to another. In other words, when redundant coordinates are used in the normal vibrational analysis, the force field becomes indeterminant. By assuming that many of the normal vibrations are relatively unperturbed, we have transferred the normal vibrational analysis using non-redundant symmetry coordinates applicable for the small molecules to the polymers. The results from such calculations have satisfactorily accounted for the observations of model compounds[20]. In the present study we have extended this technique to analyse the vibrational spectra of PPTA.

In addition, when the bands are properly assigned and reliable force constants are available, it is possible to

* To whom correspondence should be sent.
0032-3861/86/010034-13$03.00

calculate the theoretical mechanical properties[17–19] and to evaluate the stress-induced structural changes at the molecular level[12,15,16]. We have used two approaches proposed earlier[21–23] to calculate the maximum tensile modulus for PPTA. The results are reported here.

In all of these studies we have been greatly aided by analysing the vibrational spectra of deuterated molecules. Because most of the observed vibrational transitions of PPTA are unexpectedly broad, two additional model compounds have been employed, *N,N'*-phenylterephthalamide and *N,N'*-dibenzoyl-*p*-phenylene diamine, to illustrate the different environments associated with the benzene rings and the amide groups in the chemical repeat unit of PPTA. A combination of the spectra obtained for these two molecules can explain many of the features in the infra-red spectrum of PPTA. These experimental results, in conjunction with the theoretical normal vibrational analysis, are presented here.

EXPERIMENTAL

The two model compounds for PPTA, *N,N'*-phenylterephthalamide,

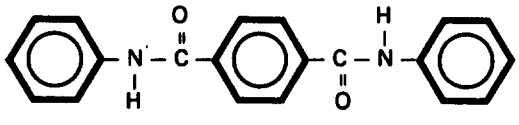

and *N,N'*-dibenzoyl-*p*-phenylene diamine

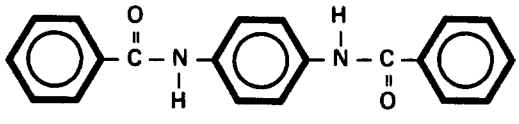

were obtained from W. W. Adams of the Air Force Materials laboratory, Ohio, USA. The *N,N'*-phenylterephthalamide was recrystallized from ethylacetoacetate and the *N,N'*-dibenzoyl-*p*-phenylene diamine was recrystallized by sublimation. Potassium bromide pellets containing 1–3% of these recrystallized samples were prepared for the infra-red measurements. Infra-red spectra were taken with an International Business Machine Model 98 vacuum Fourier transform spectrometer. Five hundred scans of 2 cm^{-1} resolution spectra were signal averaged for our analysis. Typical infra-red spectra are shown in *Figures 1* and *2*. Raman measurements were taken with a Jobin-Yvon Ramanor HG.2S spectrometer. In all cases, bandpass was maintained at 1 cm^{-1} at 5100 Å. The excitation radiation was the 5145 Å line provided by a continuous-wave Argon laser. No more than 120 mW were used in any of our measurements. Since our Raman spectrometer has very high rejection ratios in the very low frequency region, we were able to obtain the entire range (50 cm^{-1}–3600 cm^{-1}) of data for structural characterization from these powdery samples. We also attached a Cromenco microprocessor to control the spectrometer and to acquire data. The data are generally stored on 20.3 cm diskettes until transferred to an IBM 9000 computer for further analysis. The Raman spectra of the model compounds are shown in *Figures 3* and *4*. Because of the extremely small diameter (13 μm) of the as-obtained Kevlar 49 fibres, it was difficult to obtain

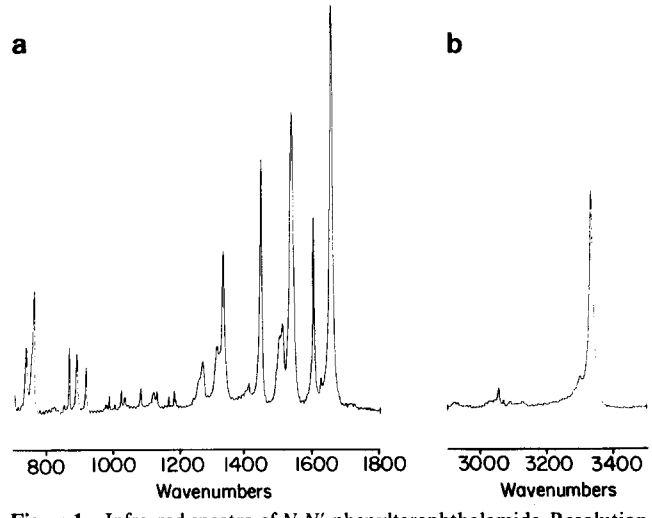

Figure 1 Infra-red spectra of *N,N'*-phenylterephthalamide. Resolution 2 cm^{-1}; 500 scans. (a) 700–1800 cm^{-1} region, (b) 2900–3500 cm^{-1} region

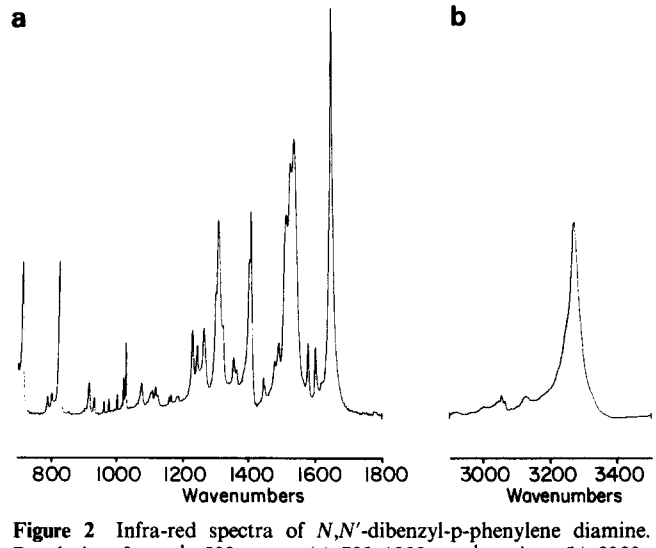

Figure 2 Infra-red spectra of *N,N'*-dibenzyl-p-phenylene diamine. Resolution 2 cm^{-1}, 500 scans. (a) 700–1800 cm^{-1} region, (b) 2900–3500 cm^{-1} region

transmission spectra without having the fibres overlap. Instead, the attenuated total reflectance technique was used. The fibres were wrapped around a germanium crystal with fibres parallel to each other and the entire assembly was dried in a vacuum oven at 100°C for 24 h. Polarized infra-red radiation was obtained by using a wire grid polarizer. The polarized spectra obtained in this fashion are shown in *Figure 5*. We encountered a considerable amount of fluorescence background in the Raman measurement of the fibres received and have elected to use the data presented in the literature[9].

In addition, we have prepared PPTA films from the as-received fibres to study the effects of the coagulants, modification of the crystalline structure, and to obtain deuterated molecules. Kevlar 29 fibres were cut into 1–2 cm long segments and dried at 150°C in vacuum for 24 h, then dissolved in 100% sulphuric acid. The polymer concentration is approximately 4–5 wt%. Thin films were prepared by smearing the solution onto glass plates and coagulating in a water/methanol mixture. To obtain deuterated films, D_2SO_4 and D_2O were used in place of H_2SO_4 and H_2O. The infra-red spectra obtained for these

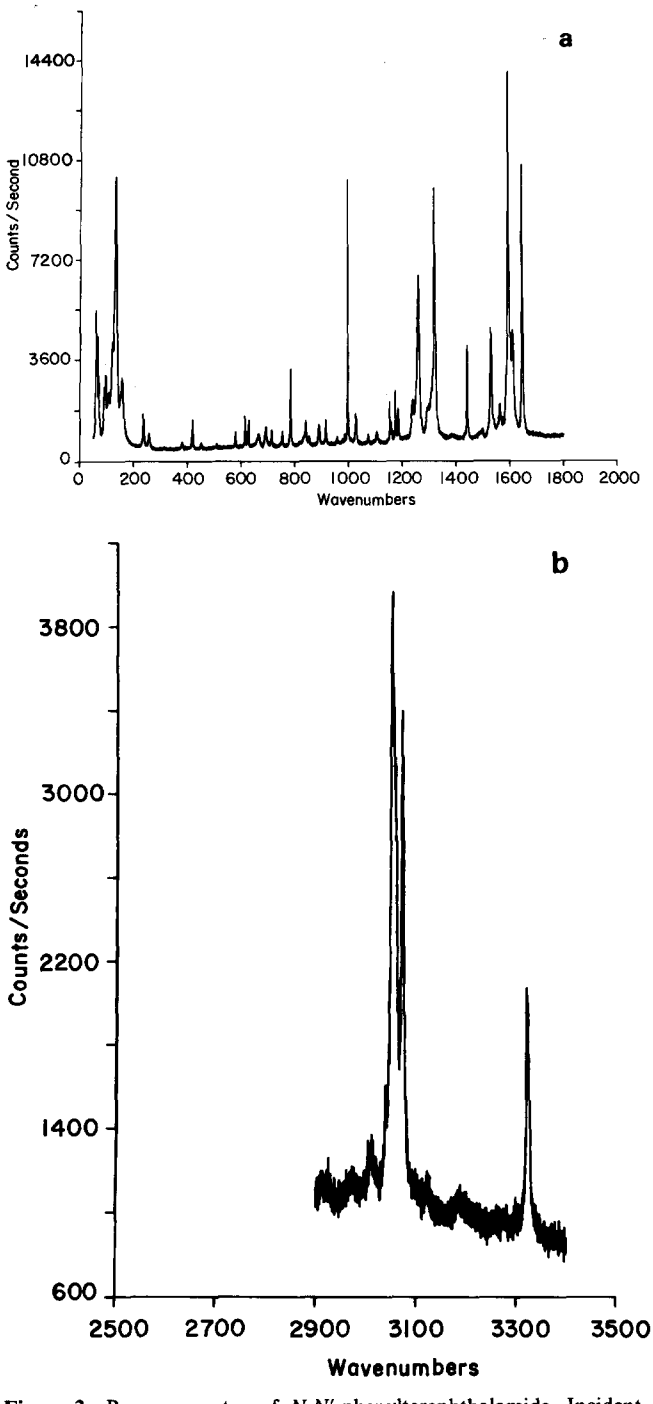

Figure 3 Raman spectra of *N,N'*-phenylterephthalamide. Incident excitation radiation 5145 Å; 1 cm^{-1} bandpass at 5100 Å. (a) 0–2000 cm^{-1} region, (b) 2500–3500 cm^{-1} region

samples are shown in *Figures 6* and *7*. Although the infra-red spectra obtained for the films are essentially identical to the fibre spectra, X-ray diffraction studies from these films exhibit no clear spacings for the films, showing a decrease in orderliness for the films we prepared. Low temperature (~100 K) infra-red spectra were also obtained for the PPTA samples using a low temperature cell constructed in our laboratory.

STRUCTURE AND FORCE FIELD

The PPTA structure used for our normal vibrational analysis is taken from X-ray diffraction studies[4] without modification. The structure deduced is in agreement with the theoretical conformational analysis of a single chain[24]. The structure is shown schematically in *Figure 8*. The structural parameters are listed in *Table 1*. The internal coordinates used in the calculation are listed in *Table 2*. The definition of the internal coordinates and the construction of non-redundant symmetry coordinates are identical to those in the previous publication on the model compound benzanilide[20]. However, in this polymer calculation, we were not able to remove the four non-vibrational motions (three translations and one rotation) from the set of non-redundant symmetry coordinates listed in *Table 3*. The main reasons for using this particular set of non-redundant coordinates are the ease in identifying the vibrational modes and the availability of the force fields developed for small molecules. In our analysis, the

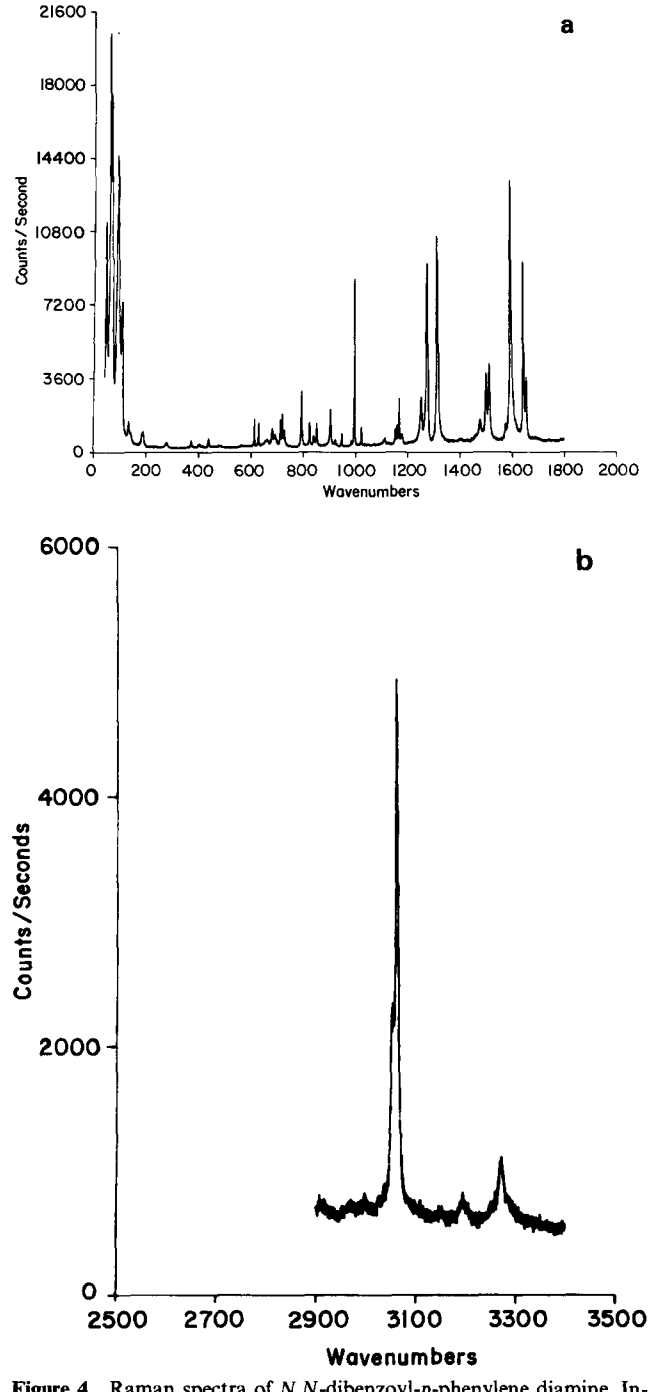

Figure 4 Raman spectra of *N,N*-dibenzoyl-*p*-phenylene diamine. Incident excitation radiation 5145 Å; 1 cm^{-1} bandpass at 5100 Å. (a) 0–2000 cm^{-1} region, (b) 2500–3500 cm^{-1} region

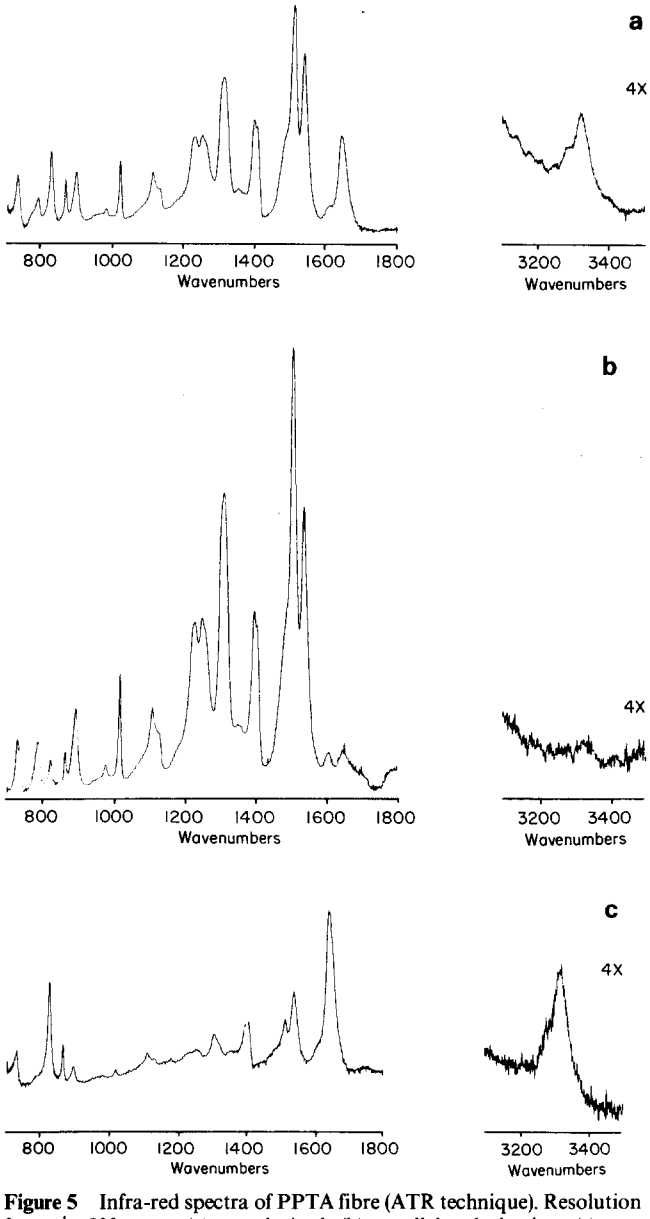

Figure 5 Infra-red spectra of PPTA fibre (ATR technique). Resolution 2 cm^{-1}; 500 scans. (a) unpolarized, (b) parallel polarization, (c) perpendicular polarization

force field associated with benzene rings was obtained from Pulay and coworkers[25]. This set was chosen since it was most complete. These values are based on *ab initio* calculations and agree quite well with the ones refined to a series of substituted benzene[26]. The force constant changes needed for PPTA due to the differences between CC'(O) and CN bonds connecting the amide group to each benzene ring were quite minor. Force constants involving the stretching, in-plane bending, and out-of-plane bending modes of these connecting bonds were taken from the corresponding values for monosubstituted benzene rings[26]. The force constants for the amide group have been transferred from the work by Dwivedi and Krimm for a series of polypeptides[27]. The entire set of force constants is listed in *Table 4*. All normal vibrational analyses were performed using Wilson's GF matrices with a set of programs modified from the earlier ones by Schatchtschneider and Snyder[28]. The observations and the calculated frequencies and the associated potential energy distributions for PPTA molecules are listed in *Tables 5* and *6*.

RESULTS AND DISCUSSION

In our analysis, since the non-redundant local symmetry coordinates are well defined, localized ring vibrational bands between 1620 and 1000 cm^{-1} can be assigned by examining the potential energy distribution in conjunction with the previous study on para-substituted benzene rings[26]. The bands in this region all have significant contributions from in-plane ring vibrational motions. Bands calculated near 1605 cm^{-1}, 1595 cm^{-1}, 1295 cm^{-1} and 1254 cm^{-1} are largely due to CC stretching modes, whereas bands calculated near 1516 cm^{-1}, 1332 cm^{-1}, 1312 cm^{-1} and 1188 cm^{-1} are largely due to CH in-plane bending modes. Other calculated bands around 1400 cm^{-1}, 1106 cm^{-1} and 1095 cm^{-1} have simi-

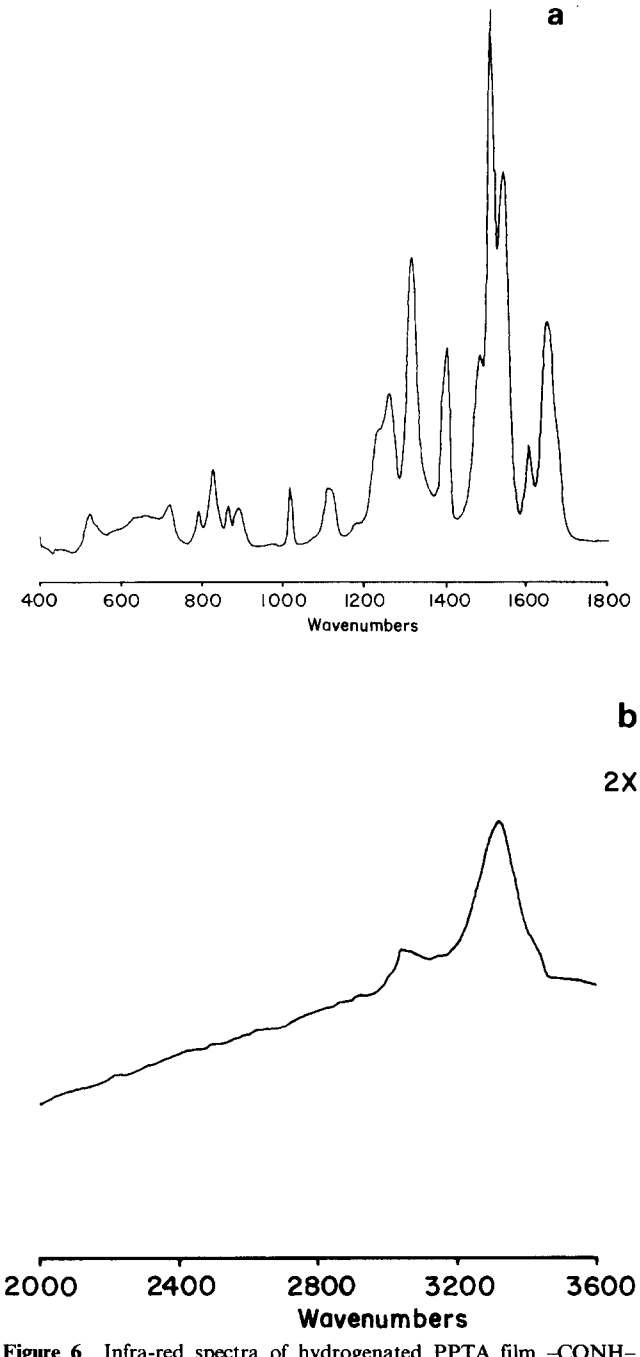

Figure 6 Infra-red spectra of hydrogenated PPTA film –CONH–. Resolution 2 cm^{-1}; 500 scans. (a) 400–1800 cm^{-1} region, (b) 2000–3600 cm^{-1} region

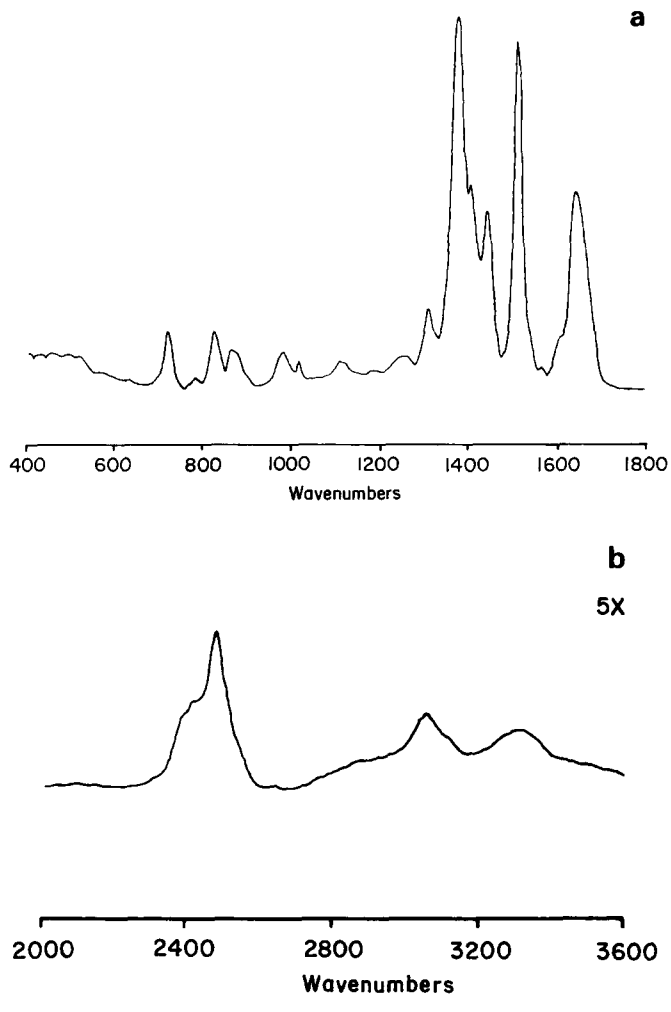

Figure 7 Infra-red spectra of deuterated PPTA film –COND–. Resolution 2 cm^{-1}; 500 scans. (a) 400–1800 cm^{-1} region, (b) 2000–3600 cm^{-1} region

lar magnitudes of contributions from both CC-stretching and CH in-plane bending modes. The band at 1014 cm^{-1} has a large contribution from the ring trigonal deformation involving deformation of the CCC angle and similar contributions from CC stretching modes. In addition to the mixing among ring CC stretching, CH in-plane bending, and ring deformation modes of one ring to the other, there are also non-negligible contributions from the amide group vibrational modes in many of the vibrations. For example, the 1495 cm^{-1} band has a large contribution from the NH in-plane bending mode. This kind of mixing from amide groups is greater than that observed for another model compound, benzanilide[20]. As expected, the difference in structure between the two parts of the chemical repeat of PPTA affects not only the character of the ring vibrations but also their frequencies as well, even though exactly the same force constants were used. Comparing vibrational modes of similar characteristics, the frequencies are generally higher for PPTA than for benzanilide, ranging from less than 5 cm^{-1} for pure modes such as the CC stretching and CH in-plane bending at 1605 cm^{-1} and 1188 cm^{-1}, respectively, to greater than 15 cm^{-1} for mixed modes at 1516 cm^{-1} and 1095 cm^{-1}. The band at 1449 cm^{-1} calculated for benzanilide disappears totally and a new band at 1400 cm^{-1} was calculated. This is due to the difference in the substituents and, in fact, similar results are observed in comparing the normal vibrational analyses of toluene and *p*-xylene[26].

Out-of-plane ring deformation modes are similarly assigned by examining potential energy distributions and comparing them with the normal coordinate analysis results of benzanilide[20] and *p*-xylene[26]. Bands in the region between 1000 and 800 cm^{-1}, for example 963 cm^{-1}, 959 cm^{-1}, 838 cm^{-1} and 824 cm^{-1} are pure enough to be positively assigned to CH out-of-plane deformation bands. But again, these bands are not completely pure. The potential energy distributions of these bands show mixing of ring out-of-plane deformations between two rings and also with amide group in-plane and out-of-plane deformation modes.

In the region below 900 cm^{-1}, most of the vibrational modes are mainly due to skeletal modes and are difficult to assign with any degree of certainty. The complexities and the lack of dominating features make the characterizations of bands below 900 cm^{-1} very difficult. For example, bands at 893 cm^{-1}, 843 cm^{-1} and 773 cm^{-1} all incorporate a considerable amount of coupling between

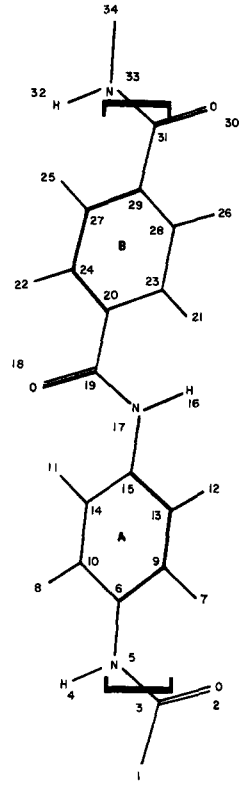

Figure 8 Schematic diagram of PPTA structure

Table 1 Structural parameters of a proposed geometry of PPTA

Length (Å)		Valence angle (°)		Dihedral angle (°)	
C–C	1.397	<(CCC)	120	τ(CCCC)	180
C–H	1.084	<(CCH)	120	τ(CCCH)	360
N–H	1.084	<(CCN)	120	$\tau(C_{23}C_{20}C'O)$	30
C–N	1.42	<(CCC′)	120	$\tau(C_{27}C_{29}C'O)$	330
N–C′	1.34	<(CNH)	120	$\tau(C_9C_6NH)$	330
C′–O	1.24	<(CNC′)	125	$\tau(C_{10}C_6NH)$	218
C′–C*	1.47	<(CC′O)	120	$\tau(C_{27}C_{29}C'N)$	150
		<(NC′C)	117	$\tau(C_{24}C_{20}C'O)$	210
				$\tau(C_{14}C_{15}NH)$	38
				$\tau(C_{14}C_{15}NC')$	218

*C′ = carbonyl carbon
C = ring carbon

Table 2 Definition of internal coordinates for PPTA

	Atoms		Atoms
Stretching			
R_1 = r(N–H)	(4,5)	R_{16} = r(C′–O)	(18,19)
R_2 = r(N–C)	(5,6)	R_{17} = r(C′–C)	(19,20)
R_3 = r(C–H)	(7,9)	R_{18} = r(C–H)	(21,23)
R_4 = r(C–H)	(12,13)	R_{19} = r(C–H)	(26,28)
R_5 = r(C–N)	(17,15)	R_{20} = r(C–C′)	(31,29)
R_6 = r(C–H)	(11,14)	R_{21} = r(C–H)	(25,27)
R_7 = r(C–H)	(8,10)	R_{22} = r(C–H)	(22,24)
R_8 = r(C–C)	(6,9)	R_{23} = r(C–C)	(20,23)
R_9 = r(C–C)	(9,13)	R_{24} = r(C–C)	(23,28)
R_{10} = r(C–C)	(13.15)	R_{25} = r(C–C)	(28,29)
R_{11} = r(C–C)	(15,14)	R_{26} = r(C–C)	(29,27)
R_{12} = r(C–C)	(14,10)	R_{27} = r(C–C)	(27,24)
R_{13} = r(C–C)	(6,10)	R_{28} = r(C–C)	(24,20)
R_{14} = r(N–H)	(16,17)	R_{29} = r(C′–O)	(30,31)
R_{15} = r(N–C′)	(17,19)	R_{30} = r(C′–N)	(31,33)
Angle bending			
	Atoms		Atoms
R_{31} = <(HNC′)	(4,5,3)	R_{55} = <(NC′O)	(17,19,18)
R_{32} = <(HNC)	(4,5,6)	R_{56} = <(OC′C)	(18,19,20)
R_{33} = <(C′NC)	(3,5,6)	R_{57} = <(CN′C)	(17,19,20)
R_{34} = <(CCN)	(10,6,5)	R_{58} = <(CCC′)	(24,20,19)
R_{35} = <(NCC)	(5,6,9)	R_{59} = <(C′CC)	(19,20,23)
R_{36} = <(CCH)	(6,9,7)	R_{60} = <(CCH)	(20,23,21)
R_{37} = <(HCC)	(7,9,13)	R_{61} = <(HCC)	(21,23,28)
R_{38} = <(CCH)	(9,13,12)	R_{62} = <(CCH)	(23,28,26)
R_{39} = <(HCC)	(12,13,15)	R_{63} = <(HCC)	(26,28,29)
R_{40} = <(CCN)	(13,15,17)	R_{64} = <(CCC′)	(28,29,31)
R_{41} = <(NCC)	(17,15,14)	R_{65} = <(C′CC)	(31,29,27)
R_{42} = <(CCH)	(15,14,11)	R_{66} = <(CCH)	(29,27,25)
R_{43} = <(HCC)	(11,14,10)	R_{67} = <(HCC)	(25,27,24)
R_{44} = <(CCH)	(14,10,8)	R_{68} = <(CCH)	(27,24,22)
R_{45} = <(HCC)	(8,10,6)	R_{69} = <(HCC)	(22,24,20)
R_{46} = <(CCC)	(10,6,9)	R_{70} = <(CCC)	(24,20,23)
R_{47} = <(CCC)	(6,9,13)	R_{71} = <(CCC)	(20,23,28)
R_{48} = <(CCC)	(9,13,15)	R_{72} = <(CCC)	(23,28,29)
R_{49} = <(CCC)	(13,15,14)	R_{73} = <(CCC)	(28,29,27)
R_{50} = <(CCC)	(15,14,10)	R_{74} = <(CCC)	(29,27,24)
R_{51} = <(CCC)	(14,10,6)	R_{75} = <(CCC)	(27,24,20)
R_{52} = <(CNH)	(15,17,16)	R_{76} = <(CC′O)	(29,31,30)
R_{53} = <(HNC′)	(16,17,19)	R_{77} = <(OC′N)	(30,31,33)
R_{54} = <(CNC′)	(15,17,19)	R_{78} = <(CC′N)	(29,31,33)
Out-of-plane bending			
	Atoms		Atoms
R_{79} = NH opb	(5,4,3,6)	R_{87} = C′O opb	(19,18,20,17)
R_{80} = CN opb	(6,5,10,9)	R_{88} = CC′ opb	(20,19,24,23)
R_{81} = CH opb	(9,7,6,13)	R_{89} = CH opb	(23,21,20,28)
R_{82} = CH opb	(13,12,9,15)	R_{90} = CH opb	(28,26,23,29)
R_{83} = CN opb	(15,17,13,14)	R_{91} = CC′ opb	(29,31,28,27)
R_{84} = CH opb	(14,11,15,10)	R_{92} = CH opb	(27,25,29,24)
R_{85} = CH opb	(10,8,14,6)	R_{93} = CH opb	(24,22,27,20)
R_{86} = NH opb	(17,16,19,15)	R_{94} = C′O opb	(31,30,29,33)
Torsion			
	Atoms		Atoms
R_{95} = C–N tor	(6,5)	R_{104} = C′–C tor	(19,20)
R_{96} = C–C tor	(6,9)	R_{105} = C–C tor	(20,23)
R_{97} = C–C tor	(9,13)	R_{106} = C–C tor	(23,18)
R_{98} = C–C tor	(13,15)	R_{107} = C–C tor	(28,29)
R_{99} = C–C tor	(15,14)	R_{108} = C–C tor	(29,27)
R_{100} = C–C tor	(14,10)	R_{109} = C–C tor	(27,24)
R_{101} = C–C tor	(10,6)	R_{110} = C–C tor	(24,20)
R_{102} = C–N tor	(15,17)	R_{111} = C–C′ tor	(29,31)
R_{103} = C′–N tor	(17,19)	R_{112} = C′–N tor	(31,33)

Table 3 Definition of local non-redundant symmetry coordinates for PPTA

	Notation	Ring A	Ring B
C–N str	r′	$S_1=R_2$	
C–C′ str	r″		$S_{43}=R_{17}$
C–H str	r	$S_2=R_3$	$S_{44}=R_{18}$
C–H str		$S_3=R_4$	$S_{45}=R_{19}$
C–N str		$S_4=R_5$	
C–C′ str			$S_{46}=R_{20}$
C–H str		$S_5=R_6$	$S_{47}=R_{21}$
C–H str		$S_6=R_7$	$S_{48}=R_{22}$
C–C str	R	$S_7=R_8$	$S_{49}=R_{23}$
C–C str		$S_8=R_9$	$S_{50}=R_{24}$
C–C str		$S_9=R_{10}$	$S_{51}=R_{25}$
C–C str		$S_{10}=R_{11}$	$S_{52}=R_{26}$
C–C str		$S_{11}=R_{12}$	$S_{53}=R_{27}$
C–C str		$S_{12}=R_{13}$	$S_{54}=R_{28}$
CN ipb	β'	$S_{13}=(R_{35}-R_{34})/2^{1/2}$	
CC′ ipb	β''		$S_{55}=(R_{59}-R_{58})/2^{1/2}$
CH ipb	β	$S_{14}=(R_{37}-R_{36})/2^{1/2}$	$S_{56}=(R_{61}-R_{60})/2^{1/2}$
CH ibp		$S_{15}=(R_{39}-R_{38})/2^{1/2}$	$S_{57}=(R_{63}-R_{62})/2^{1/2}$
CN ipb		$S_{16}=(R_{41}-R_{40})/2^{1/2}$	
CC′ ipb			$S_{58}=(R_{65}-R_{64})/2^{1/2}$
CH ipb		$S_{17}=(R_{43}-R_{42})/2^{1/2}$	$S_{59}=(R_{67}-R_{66})/2^{1/2}$
CH ipb		$S_{18}=(R_{45}-R_{44})/2^{1/2}$	$S_{60}=(R_{69}-R_{68})/2^{1/2}$
trigonal def.	q_{19}	$S_{19}=(R_{46}-R_{47}+R_{48}-R_{49}+R_{50}-R_{51})/6^{1/2}$	$S_{61}=(R_{70}-R_{71}+R_{72}-R_{73}+R_{74}-R_{75})/6^{1/2}$
asy def A	q_{20}	$S_{20}=(2R_{46}-R_{47}-R_{48}+2R_{49}-R_{50}-R_{51})/12^{1/2}$	$S_{62}=(2R_{70}-R_{71}-R_{72}+2R_{73}-R_{74}-R_{75})/12^{1/2}$
asy def B	q_{21}	$S_{21}=(R_{47}-R_{48}+R_{50}-R_{51})/2$	$S_{63}=(R_{71}-R_{72}+R_{74}-R_{75})/2$
CN opb	γ'	$S_{22}=R_{80}$	
CC′ opb	γ''		$S_{64}=R_{88}$
CH opb	γ	$S_{23}=R_{81}$	$S_{65}=R_{89}$
CH opb		$S_{24}=R_{82}$	$S_{66}=R_{90}$
CN opb		$S_{25}=R_{83}$	
CC′ opb			$S_{67}=R_{91}$
CH opb		$S_{26}=R_{84}$	$S_{68}=R_{92}$
CH opb		$S_{27}=R_{85}$	$S_{69}=R_{93}$
puckering	q_{28}	$S_{28}=(R_{96}-R_{97}+R_{98}-R_{99}+R_{100}-R_{101})/6^{1/2}$	$S_{70}=(R_{105}-R_{106}+R_{107}-R_{108}+R_{109}-R_{110})/6^{1/2}$
asy tor A	q_{29}	$S_{29}=(-R_{96}+R_{98}-R_{99}+R_{101})/2$	$S_{71}=(-R_{105}+R_{107}-R_{108}+R_{110})/2$
asy tor B	q_{30}	$S_{30}=(-R_{96}+2R_{97}-R_{98}-R_{99}+2R_{100}-R_{101})/12^{1/2}$	$S_{72}=(-R_{105}+2R_{106}-R_{107}-R_{108}+2R_{109}-R_{110})/12^{1/2}$
N–H str	t	$S_{31}=R_{14}$	$R_{73}=R_1$
N–C′	R′	$S_{32}=R_{15}$	$S_{74}=R_{30}$
C′–O str	S	$S_{33}=R_{16}$	$S_{75}=R_{29}$
NH opb	μ	$S_{34}=R_{86}$	$S_{76}=R_{79}$
C′O opb	μ'	$S_{35}=R_{87}$	$S_{77}=R_{94}$
CC′N def	δ'	$S_{36}=(2R_{57}-R_{56}-R_{55})/6^{1/2}$	$S_{78}=(2R_{78}-R_{77}-R_{76})/6^{1/2}$
C′O ipb	θ'	$S_{37}=(R_{56}-R_{55})/2^{1/2}$	$S_{79}=(R_{76}-R_{77})/2^{1/2}$
C′NC def	δ	$S_{38}=(2R_{54}-R_{53}-R_{52})/6^{1/2}$	$S_{80}=(2R_{33}-R_{32}-R_{31})/6^{1/2}$
NH ipb	θ	$S_{39}=(R_{53}-R_{52})/2^{1/2}$	$S_{81}=(R_{31}-R_{32})/2^{1/2}$
CN tor	τ_1	$S_{40}=R_{102}$	$S_{82}=R_{95}$
NC′ tor	τ_2	$S_{41}=R_{103}$	$S_{83}=R_{112}$
C′C tor	τ_3	$S_{42}=R_{104}$	$S_{84}=R_{111}$

the in-plane vibration of the ring and the out-of-plane vibrations of the ring and the amide group.

The assignments for the amide bands are greatly assisted by the deuteration experiment. By following the disappearance of the NH stretching and the appearance of the ND bands in the 3300 cm^{-1} and 2400 cm^{-1} regions, respectively, it can be established that all the amide groups have been deuterated. It is interesting to note, however, that the NH band will re-emerge as a function of time when the film is simply exposed to air. The spectroscopic changes as a function of time are shown in *Figure 9*. It has been suggested that one of the deficiencies associated with PPTA is its propensity to absorb water[29]. We found that this is certainly true and, in fact, occurred readily for the samples we prepared. Since the decrease in the intensity of the N–H stretching vibration is proportional to the number of N–D units around, the diffusion of the H_2O molecules can be followed by measuring the relative intensity of the two bands in the 3300 cm^{-1} and 2400 cm^{-1} regions. We recognize that this type of measurement is only an approximation since the absolute intensity of these vibrations do differ depending on the strength of the hydrogen bonds formed[30]. By using this spectroscopic technique, it was established previously that the diffusion rate depends greatly on the orderliness of interchain packing[31]. In that study, Nakanishi *et al.* found that the N–H and N–D conversion rates differ by a factor of 10 or more between the helical and random coil conformation of poly-L-glutamic acid. For the 8 μm thick film used in this study, there was an increase in the N–H content by a factor of three after four days at room temperature. The rate of change is shown in *Table 7*.

The amide bands, especially those in the higher frequency range, are quite easily assigned by following the deuteration experiment. Because of the chemically different environments between the two amide groups in the repeat unit of PPTA, we expect the degeneracy of the

Table 4 Force constants for PPTA

Force constant	Value	Force constant	Value
(a) phenyl group			
K(r)	5.104	$F(R)^o$	0.633
K(r′)	5.043	$F(R)^m$	−0.442
K(r″)	4.409	$F(R)^p$	0.440
K(R)	6.500	$F(R_1\beta_1)$	0.167
K(β)	0.512	$F(R_1\beta_3)$	−0.010
H(β')	0.8375	$F(R_1\beta_4)$	0.019
H(β'')	0.8375	$F(R_1q_{20})$	0.134
$H(q_{19})$	1.236	$F(R_2q_{20})$	−0.268
$H(q_{20})$	1.236	$F(R_3q_{20})$	−0.067
$H(q_{20})$	1.236	$F(R_1q_{21})$	0.2321
H(γ)	0.5852	$F(R_3q_{21})$	−0.2321
H(γ')	0.6581	$F(\beta)^o$	0.009
H(γ'')	0.6581	$F(\beta)^m$	0.010
$H(q_{28})$	0.3763	$F(\beta)^p$	−0.001
$H(q_{29})$	0.3156	$F(\beta_2q_{20})$	−0.067
$H(q_{30})$	0.3156	$F(\beta'q_{21})$	0.07736
$F(r)^o$	0.016	$F(\beta''q_{21})$	0.07736
$F(r)^m$	0.005	$F(\beta_2q_{21})$	0.03863
$F(r)^p$	0.001	$F(\gamma)^o$	−0.092
$F(r_1R_1)$	0.079	$F(\gamma)^m$	−0.0004
$F(r_1R_2)$	−0.002	$F(\gamma)^p$	−0.0235
$F(r_1R_3)$	−0.022	$F(\gamma_1q_{28})$	−0.1681
$F(r_1\beta_2)$	0.005	$F(\gamma_2q_{28})$	0.1681
$F(r_1\beta_3)$	−0.007	$F(\gamma'q_{29})$	0.1700
$F(r_1q_{19})$	−0.105	$F(\gamma''q_{29})$	0.1700
$F(r_2q_{19})$	0.105	$F(\gamma_2q_{29})$	−0.0850
$F(r'q_{19})$	0.105	$F(\gamma_2q_{30})$	−0.1472
$F(r''q_{19})$	−0.105	$F(\gamma_3q_{30})$	0.1472
$F(r_2q_{20})$	0.0495	$F(r'R_1)$	0.3
$F(r'q_{20})$	−0.099	$F(r''R_1)$	0.2506
$F(r''q_{20})$	−0.099	$F(R_1\beta')$	0.220
		$F(R_1\beta'')$	0.220
(b) amide group			
K(t)	6.168	$F(R'\theta')$	−0.1414
K(R′)	6.415	$F(R'\delta)$	0.1249
K(S)	9.582	$F(R'\delta')$	0.1633
H(θ)	0.6205	$F(S\delta')$	−0.4899
H(δ)	0.6625	$F(r''\theta')$	0.1414
H(θ')	1.246	$F(r''\delta')$	0.1633
H(δ')	1.3487	$F(r'\theta)$	−0.2079
H(μ)	0.129	$F(r'\delta')$	0.1249
H(μ')	0.587	$F(\theta\theta')$	−0.1255
H(τ_1)	0.010	$F(\delta\delta')$	−0.0248
H(τ_2)	0.680	$F(\theta'\delta)$	0.0725
H(τ_3)	0.010	$F(\theta\delta')$	0.043
F(γ'R′)	0.300	$F(\theta\delta)$	0.0231
F(R′S)	0.500	$F(\mu\mu')$	0.010
F(r″R′)	0.300	$F(\mu'\tau_2)$	0.011
F(r″S)	0.500	$F(\mu\tau_2)$	−0.1677
F(R′θ)	0.2079		

amide vibrations to be lifted. This is true in the calculation but is not reproduced accurately in the experiment. Two bands at 1675 cm^{-1} and 1654 cm^{-1} have been calculated as the two Amide I bands associated with the chemical repeat unit of PPTA. These two bands were calculated to be 1672 cm^{-1} and 1651 cm^{-1} in the deuterated molecule, essentially unshifted from the original positions. This is to be expected since Amide I vibration does not involve significant NH contributions. The Amide I bands observed in PPTA and deuterated species are at 1650 cm^{-1} and 1645 cm^{-1}, respectively. These two bands are fairly broad, approximately 20 cm^{-1} in width. Even in the spectrum obtained at liquid nitrogen temperature, no evidence of the splitting was observed. However, at lower measurement temperatures the asymmetry of this Amide I band is enhanced.

Calculated Amide II bands at 1567 cm^{-1} and 1528 cm^{-1} are shifted considerably to 1473 cm^{-1} and 1447 cm^{-1}, respectively, upon deuteration. Therefore, the band observed at 1539 cm^{-1} is assigned to the Amide II vibration. Because of the significant NH in-plane bending contribution, it shifted to 1446 cm^{-1} upon deuteration, close to the predicted value. Similarly, the band observed at 1259 cm^{-1} can be assigned to the Amide III vibration, since it shifted to 982 cm^{-1} in deuterated PPTA. The calculated Amide III bands are at 1283 cm^{-1} and 1254 cm^{-1} for PPTA and at 978 and 966 cm^{-1} in deuterated PPTA. These assignments are consistent with the polarization measurements since Amide I is expected to be perpendicularly polarized and Amide II and III are polarized in the parallel direction with respect to the chain direction as seen in *Figure 5*.

Perhaps one of the most fascinating aspects of the Kevlar spectrum is the considerable width observed for the infra-red and Raman bands. All the bandwidths observed for the model compounds are approximately half of the values observed for the polymer. Several factors increase the width of a vibrational band, including the conformational distribution and lack of interchain order, especially the specificity and magnitude of hydrogen bonding in PPTA. The diffraction studies led to the conclusion that PPTA fibres are of essentially 100% crystallinity[8] containing few conformational or packing disorders. Undoubtedly, because of differences in the chemical structure and environments, we expect different frequencies to exist for both amide groups and benzene rings, and especially for vibrational modes coupled to the backbone. In a similar case, we have already seen the calculated and observed differences for the two rings in benzanilide. Therefore, guided by the vibrational analysis, we began to examine whether the vibrational spectrum of Kevlar is actually a sum of the two model compounds. We paid particular attention to the regions near bands at 3320 cm^{-1}, 1400 cm^{-1}, 1310 cm^{-1}, 1260 cm^{-1} and 1230 cm^{-1}. Excluding the obvious bands which arise from the mono-substituted benzene rings, for example the ones near 1441 cm^{-1}, 1076 cm^{-1} and 1000 cm^{-1}, the broad bands observed for PPTA can indeed be constructed from the spectra obtained for the two model compounds as shown in *Figure 10*.

It is particularly fascinating to note the rather large difference between the NH stretching vibration for the two model compounds, one at 3279 cm^{-1} and the other at 3340 cm^{-1}. This vibrational mode is very localized in nature, the difference is really due to the difference in the physical environment, i.e. the magnitude and specificity of the hydrogen bonds formed. We have assigned the broad NH stretching vibration (halfwidth ~100 cm^{-1}) found in PPTA to be associated mainly with the two different units in the repeat unit rather than assigning the broad bandshape strictly to poorly defined hydrogen bonds formed in association with ill-defined structures.

The generally broad features of bands assigned to the amide group (1650 cm^{-1}, 1539 cm^{-1} or 1259 cm^{-1}), or likewise those assigned to the ring vibrations (around 1610 cm^{-1}, 1510 cm^{-1}, 1360–1420 cm^{-1} and 1308 cm^{-1}) can be confidently attributed to the influence of different sections of the repeat unit of PPTA.

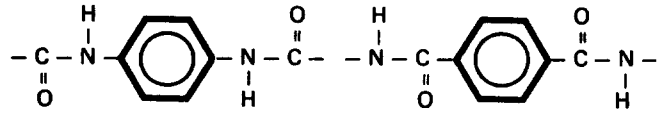

Table 5 Observed and calculated frequencies (in cm^{-1}) of PPTA

i.r.[a]	Raman[c]	Calculated	Potential energy distribution[d]	i.r.		Calculated	Potential energy distribution
3324		3344	17A(92)	864		853	7B(64), 9B(17), 16A(11), 16B(11), 21A(5)
		3344	17B(92)				
		3062	1A(99)			843	2A(21), 5B(8), 9A(7)
		3062	1B(99)			838	7B(112)
		3059	1A(99)			838	7A(112)
		3059	1B(100)	823		824	7A(24), 8B(16), 13B(9), 8A(9), 27B(6), 16B(6)
3041		3040	1A(100)				
		3040	1B(99)			811	7A(48), 8B(22), 10A(7), 16B(7), 13B(7), 16A(5)
		3039	1A(100)				
		3039	1B(99)	787	789	773	8A(69), 8B(23), 13A(17), 13B(14), 16A(6), 16B(6)
		1675	19A(44), 18A(22), 22A(9)				
1650	1649	1654	19B(59), 18B(16), 22B(12), 19A(9)			746	4A(23), 11B(12), 11A(10)
	1615	1615	2A(19), 2B(11), 19A(10), 14B(7)	728	734	725	5B(32), 23A(7), 23B(6)
1610		1605	2B(40), 2A(24), 5A(6), 5B(6)		698	694	7B(39), 21A(30), 21B(16), 16A(6)
		1595	2A(52), 3A(13), 6A(6), 25A(5)	668[b]		682	8A(32), 21B(27), 8B(17), 20B(10), 13A(6)
		1580	2B(29), 25B(11), 19B(9), 18A(8), 2A(6), 3B(6)			661	8B(20), 7A(10), 13A(8), 27B(8), 21A(8), 20A(6)
	1570	1567	2B(31), 19A(13), 25A(11), 18B(7), 3B(7), 14B(5)		632	646	6B(67), 6A(12)
1539		1528	25B(17), 18B(14), 25A(12), 2B(7), 14B(6), 18A(5)			637	6A(59), 6B(13)
						581	8A(34), 27A(18), 20A(16), 8B(11)
1510	1518	1516	3A(43), 2A(26), 11B(7)			565	8B(34), 5A(25), 22B(11), 22A(8)
1484		1495	3B(40), 25B(15), 2B(14)			545	9B(20), 9A(15), 16B(10), 16A(9), 13A(10), 13B(9)
1406	1409	1400	3A(25), 2A(21), 3B(5)				
1396		1391	3B(31), 2B(22)	445		450	9A(44), 13B(15), 13A(14), 16A(12), 16B(9)
	1331	1332	3B(29), 3A(24), 25A(7), 2B(6), 14B(6)				
1308		1318	2A(44), 3A(24), 25B(9), 3B(7), 14A(6)	420		428	5A(16), 5B(13), 12A(6), 15B(6), 12B(6)
		1312	3B(37), 3A(25), 2A(5)				
		1295	2B(112), 3B(6)			421	9B(49), 16A(15), 16B(14), 5A(10), 20A,(6)
	1279	1283	25B(17), 25A(13), 3A(8), 11A(6), 2A(5)			401	10B(131), 10A(30)
						401	10A(131), 10B(30)
1259		1254	2A(92), 25B(8), 25A(7), 4A(6)				
		1241	11B(15), 2B(12), 14A(8), 11A(9), 14B(7), 4B(8)	346		343	12A(15), 12B(13), 5A(10), 23B(7), 23A(7), 5B(6)
1226		1226	11A(19), 2A(15), 11B(15), 14B(10), 14A(7)			328	9B(21), 33B(14), 22A(14), 11A(6)
						312	20A(46), 27A(9), 13B(6), 13A(6)
	1192	1188	3B(76)			279	20B(24), 12B(17), 24A(13), 13B(11), 9A(9)
1130	1187	1187	3A(74)				
1109	1104	1106	3B(27), 2B(16), 4B(12), 18B(5)	252		258	15B(22), 15A(16), 21A(9), 13A(7) 21B(6)
		1101	3A(50), 2A(36)				
		1095	3B(26), 2B(22), 4B(7), 18B(7)			242	15A(16), 23B(11), 16B(10), 6B(8), 24B(8)
		1074	3B(27), 18A(12), 18B(7)				
1017		1014	4A(35), 2A(32)			218	20B(53), 27B(33), 9A(16), 21B(8)
		1013	4B(43), 2A(28)			102	15B(25), 15A(22), 9A(18)
979		963	7B(124), 10B(11)			93	27A(19), 19B(18), 12A(18), 16A(11), 13A(6)
		963	7A(124), 10A(11)				
		959	7B(65), 7A(64), 8B(28), 8A(27)			87	27B(50), 20B(22), 16B(12), 12B(11), 9B(9)
		953	7B(68), 7A(66), 8B(23), 8A(22)				
894		893	7A(16), 13B(10), 9A(9), 24B(9), 22B(7)			75	24B(23), 24A(23), 22A(9), 22B(8)
						28	28A(25), 28B(24), 26B(23), 26A(22)
		883	24A(11), 22A(9), 19A(6), 23A(5), 24B(5)			22	26B(24), 28A(22), 26A(20), 28B(16)
						19	26A(28), 28A(27), 26B(22), 28A(22)

[a] Observed frequencies are from the ATR spectrum of Kevlar fibre.
[b] Observed frequencies below 700 cm^{-1} are obtained from mid- and far-i.r. spectra of PPTA films.
[c] Raman data is from ref. 9.
[d] Number of the coordinate is followed by the potential energy in per cent. Contributions less than 5% are not included. The coordinate definitions in potential energy distribution are:

1 ring C–H stretching
2 ring C–C stretching
3 ring C–H in-plane bending
4 ring trigonal deformation
5 ring asymmetric deformation—type 1
6 ring asymmetric deformation—type 2
7 ring C–H out-of-plane bending
8 ring puckering
9 ring asymmetric torsion—type 1
10 ring asymmetric torsion—type 2
11 C–N stretching
12 C–N in-plane bending
13 C–N out-of-plane bending
14 C′–C stretching
15 C′–C in-plane bending
16 C′–C out-of-plane bending
17 N–H(D) stretching
18 N–C′ stretching
19 C′–O stretching
20 N–H(D) out-of-plane bending
21 C′–O out-of-plane bending
22 NC′C bending
23 C′–O in-plane bending
24 CNC′ bending
25 N–H(D) in-plane bending
26 CN torsion
27 NC′ torsion
28 C′C torsion

A and B distinguish two amide groups and two benzene rings as shown below

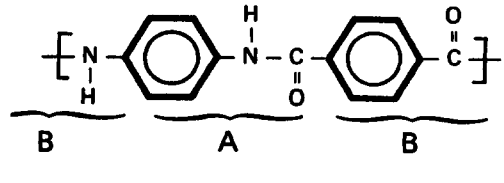

Table 6 Observed and calculated frequencies (in cm^{-1}) of deuterated PPTA (–NDCO–)

Infra-red	Calculated	Potential energy distribution[a]	i.r.	Calculated	Potential energy distribution
	3062	1A(81)		948	7A(80), 8A(21), 7B(24), 25B(12)
	3062	9B(80)		882	7B(22), 7A(14), 10B(9), 13B(8), 9A(8), 16B(7)
	3059	1A(99)	863	869	22A(8), 24B(7), 24A(7), 22B(5)
	3059	1B(99)		844	7B(50), 16B(11), 10B(11)
	3040	1A(94)		838	7B(88), 7A(24)
	3040	1B(94)		838	7A(88), 7B(24)
	3039	1B(96)	825	831	8B(11), 16A(6)
	3039	1B(96)		816	8B(21), 16B(6), 16A(6), 8A(6)
	2462	17A(98)		808	7A(50), 8B(14), 9A(7)
2475	2462	17B(98)		769	8A(78), 8B(21), 13A(17), 13B(16)
	1672	19A(45), 18A(20), 22A(9)		726	4A(15), 11B(10), 6B(7), 11A(6)
1645	1651	19B(56), 18B(16), 22A(9), 19A(11)	719	719	6B(25), 23A(10)
	1609	2A(36), 2B(14), 5A(8)		692	7B(36), 21A(29), 21B(18)
1605	1606	2B(48), 2A(19), 5B(7)		676	8B(31), 21B(28), 8A(21)
	1587	2A(79), 6A(10)		650	6A(15), 17B(10), 7A(10), 13A(9), 8B(7)
1565	1578	2B(57), 19B(13)		645	6B(63), 6A(6)
	1543	14B(17), 11A(13), 18A(11)		636	6A(53), 6B(13)
1514	1515	3A(29), 3B(18), 2A(15)		570	8A(34), 27A(20), 8B(12), 20A(11)
	1473	18A(30), 14B(15), 23A(12), 25A(8)		553	8B(26), 5A(23), 22B(14)
1446	1447	3B(16), 18A(14), 25B(7), 23B(6)		541	10B(21), 9A(14), 16B(10), 16A(10), 13A(9)
1407	1399	3A(36), 2A(26)		444	9A(32), 10B(12), 23A(14), 23B(10), 13A(10), 13B(10)
1379	1389	3B(35), 2B(25)			
	1321	3B(58), 3A(11)		425	5A(16), 6B(13), 12A(6), 15A(5)
1310	1312	3A(51), 3B(34)		413	9B(38), 9A(21), 16A(11), 16B(10)
	1294	2B(140)		401	10A(141), 7A(24), 10B(19)
	1287	2A(152)		401	10B(142), 7B(24), 10A(19)
1254	1240	11B(17), 4A(16), 11A(11), 4B(7), 14B(7), 14A(6)		338	12A(12), 12B(12), 5A(11), 5B(7), 23B(8), 23A(7)
	1227	11A(18), 11B(17), 14A(10), 14B(6), 2A(15)		326	9B(22), 22B(14), 22(14)
1183	1188	3B(54), 3A(25)		270	9A(20), 24A(15), 24B(13), 20A(8), 23A(8), 12B(8)
	1187	3A(52), 3B(25)			
	1151	4B(18), 4A(10), 25A(8)		262	13B(13), 13A(11), 15B(10), 15A(9)
	1125	2B(18), 25B(9), 25A(7), 14B(8)		249	20A(13), 15B(12), 15A(11), 5B(9), 23B(8)
1109	1101	2A(26), 3A(35), 3B(10)		231	20A(34), 16B(13), 21A(12)
	1100	2B(26), 3B(34), 2A(11)		180	20B(65), 27B(26)
1017	1014	4B(20), 4A(17), 2B(11)		101	15A(24), 15B(22), 9A(19)
	1014	4A(23), 4B(19), 2A(10)		92	9B(24), 12A(18), 27A(12), 12B(9)
982	978	25A(42), 23A(12), 8A(9)		82	27B(59), 29B(34), 27A(12), 12B(9)
	966	25B(45), 8A(15), 7A(26)		74	24B(23), 24A(23), 22A(9), 22B(23)
	963	7B(64), 7A(62)		28	28A(25), 28B(24), 26A(23), 26B(23)
	963	7A(64), 7B(62)		22	26B(22), 26A(21), 28B(19), 28A(19)
	957	7B(106), 8B(42)		20	26B(25), 26A(25), 28A(25), 28B(25)

[a] For notation of coordinates used in potential energy distribution, see footnotes to *Table 5*.

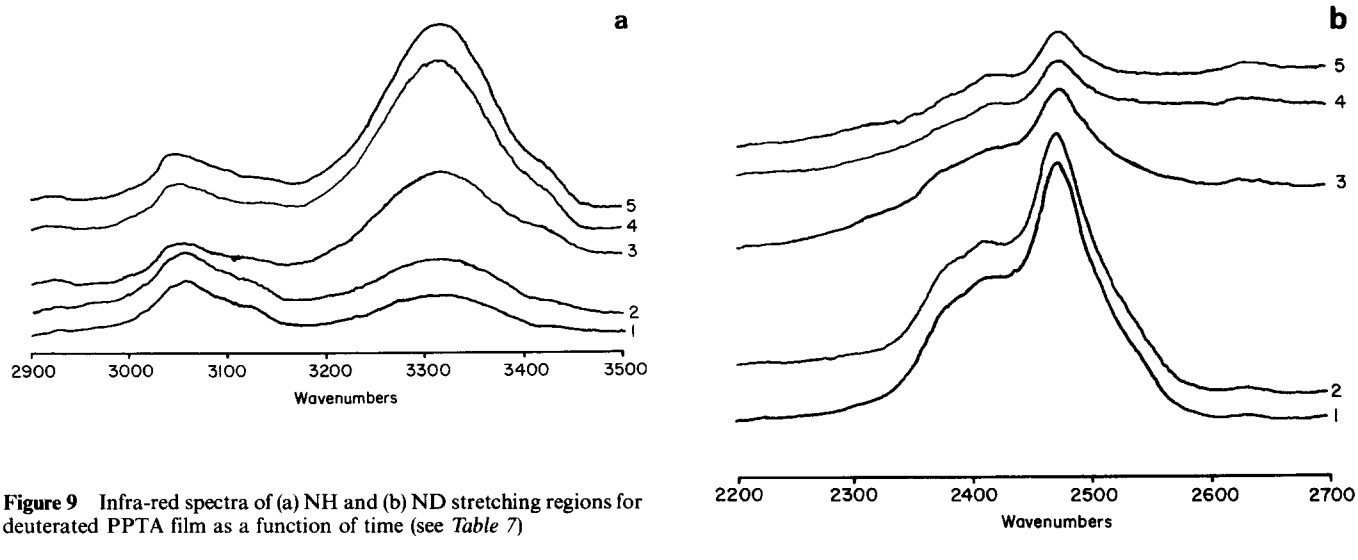

Figure 9 Infra-red spectra of (a) NH and (b) ND stretching regions for deuterated PPTA film as a function of time (see *Table 7*)

Table 7 Changes of NH and ND stretching band intensities of a deuterated PPTA film

Spectrum	Drying conditions: Time (day)	Drying conditions: Temperature (°C)	Ratioed band intensity: NH	Ratioed band intensity: ND
1	0.5	22	1	1
2	1.5	22	1.45	0.95
3	4	22	3.53	0.44
4	4	22	5.83	0.30
	1	90		
5	4	22	6.26	0.22
	2	90		

This conclusion can be demonstrated most clearly by adding the spectra of the two model compounds, as shown in *Figure 10*. The absolute intensities of the two model compounds do differ. However, there is no doubt that the overall contour and width of the bands observed in Kevlar are well reproduced by the sum of the two spectra.

MODULUS CALCULATION

As mentioned earlier, the significant interest shown in PPTA is due to its extremely high modulus and strength. However, because of the complexity of its morphology, the tensile modulus may be lower than the ultimate one. Therefore, a reliable estimate will be quite important. Several attempts have been made using various force fields suitable for the individual components of the PPTA structures[22,23]. First, the ultimate elastic modulus of PPTA in the direction of the chain axis is calculated by a method described by Treloar[21] using the force constants associated with our analysis. In this calculation, the PPTA chain is assumed to lie in one plane so that there will be no contribution from torsional deformation of the chain to the elastic modulus, although PPTA actually exists in a non-planar configuration with a dihedral angle of 30° between the phenyl ring and the amide group. For simplicity, the calculation of the overall strain of a polymer chain was carried out in three parts: bond stretching, valence angle deformation of the repeat unit excluding the benzene ring, and the overall deformation of the benzene ring itself. Therefore, the combined length of increment, ΔL, per unit applied force, F, $\frac{\Delta L}{F}$, is

$$\frac{\Delta L}{F}=\frac{\Delta L_{BS}}{F}+\frac{\Delta L_{VA}}{F}+\frac{\Delta L_{BR}}{F}$$

where ΔL_{BS}, ΔL_{VA} and ΔL_{BR} are the length increments due to the bond stretchings, valence angle deformation and benzene rings of each repeat unit, respectively. The modulus is then calculated from the following equation:

$$E=\left(\frac{F}{A}\right)\Big/\left(\frac{\Delta L}{L}\right)$$

where A is the cross sectional area and L is the repeat unit length of a chain. A cross sectional area of 20.38 Å^2 and repeat unit length of 12.89 Å have been taken from X-ray diffraction studies[4]. Our calculated ultimate elastic modulus of PPTA is 184 GPa.

Of the total deformation of a repeat unit, 28% is due to bond stretching, 38% is due to valence angle deformation excluding the benzene ring, and 34% is due to the benzene ring deformation. Although this modulus value is higher than the observed macroscopic modulus for PPTA fibre (Kevlar 49) of 128 GPa, it is less than the elastic modulus in the crystalline region in the chain direction, which was found to be 200 GPa[32]. This low calculated value of the ultimate modulus is probably due to the intrinsic discrepancies that exist in the calculation method used above, including the complete neglect of cross terms of force constants (interaction force constants).

In order to overcome this difficulty in incorporating cross interaction terms, the modulus, E, of a chain polymer can also be obtained from the frequency of the

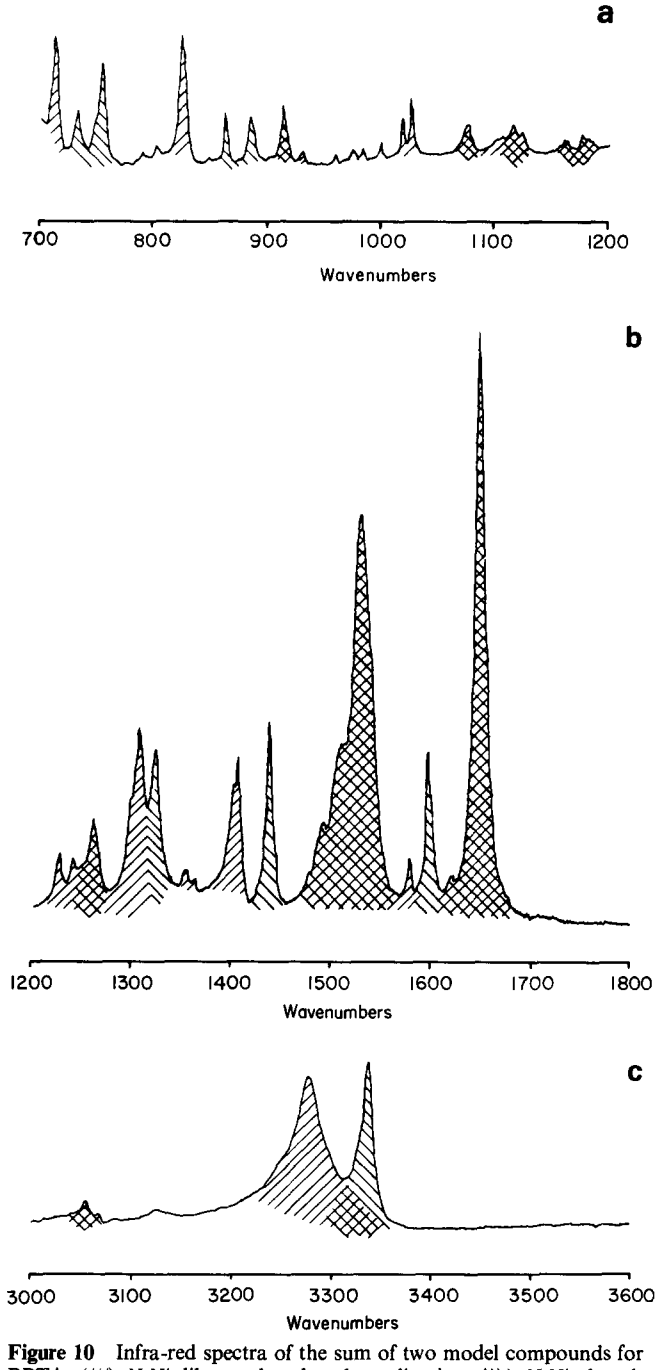

Figure 10 Infra-red spectra of the sum of two model compounds for PPTA. (///) *N,N'*-dibenzoyl-*p*-phenylene diamine, (\\\) *N,N'*-phenyl-terephthalamide. (a) 700–1200 cm^{-1} region, (b) 1200–1800 cm^{-1} region, (c) 3000–3600 cm^{-1} region

longitudinal acoustic mode (LAM) through the following relation:

$$v=\frac{1}{2cL}\sqrt{\frac{E}{\rho}}$$

where L is the chain length, c is the speed of light and ρ is the density of the polymer. For a real polymer, L is too long for normal coordinate analysis to calculate the LAM frequency directly. Therefore, we have to utilize the symmetry of an infinite polymer chain to get the dispersion curve of this LAM vibration. The slope of this dispersion curve at the zone centre ($k=0$) is proportional to the modulus E. In this way, we can fully use our force constants deduced from the spectra and at the same time take the non-planar conformation into consideration.

The dispersion curve is obtained by calculating the LAM frequency of an infinitely long PPTA chain at various phase angles. The result is given in *Table 8*. Using the density of 1.50 g cm^{-1},[5] we then obtained the modulus of 241 GPa. This value is higher than those obtained by Tashiro *et al.*[24] and by Fielding-Russell[22]. In their calculation, force constants have been transferred from similar chemical structures. However, the values were refined using a set of coordinates containing redundancies, making them less reliable. Our force constants are transferred from the model compounds and refined for non-redundant coordinates and should be more reliable. However, the modulus calculation is only applicable for an isolated polymer chain. In a real polymer, the chain would form strong hydrogen bonds with adjacent chains in the crystal. In general, these intermolecular interactions would increase the modulus even further.

CONCLUSION

We have analysed the vibrational spectra of poly(*p*-phenylene terephthalamide). The structure used is identical to the one obtained by the X-ray diffraction method and all the internal coordinates have been defined as was done previously in the analysis of the model compound benzanilide. In order to take advantage of the well-defined force field developed for either the benzene ring or the amide group, a specific set of non-redundant symmetry coordinates was used in our normal vibrational calculation. Even though no refinement was carried out in the present analysis, satisfactory assignments were made for the observed bands in the region above 800 cm^{-1}. The mostly delocalized vibrations observed in the lower frequency regions were not analysed. The analysis was greatly aided by the polarized spectra obtained for the commercial Kevlar 49 fibres. Some thin films were also prepared in our study, even though both X-ray and vibrational analysis indicate that the degree of order and orientation are significantly lower than in the original fibres. Because of the chemical and physical differences of the two benzene rings and amide groups within each translational repeat of PPTA, we expected and calculated two nearly degenerate vibrations of the mostly delocalized vibrations in the region studied. Since two model compounds representative of each unit are available (*N,N'*-phenylterephthalamide and *N,N'*-dibenzoyl-*p*-phenylene diamine), it was extremely interesting to compare the individual spectra and their sum to the infra-red spectrum obtained for PPTA. Initially we were very surprised by the poorly defined spectroscopic features found for PPTA, considering that all previous analyses have suggested that the fibre sample is essentially 100% crystalline. Guided by our calculations and the comparison between the spectra found for the two model compounds to PPTA, virtually all the broad features found for the polymer were satisfactorily explained. Our previous study as well as others has shown that both the frequency and intensity of PPTA bands will be sensitive to externally applied stress. Our present analysis shows it would be misleading to simply use the change in frequency of a broad contour to deduce conformational change due to the application of external stress, or, in fact, for other microstructural characterization purposes.

Table 8 Results of LAM calculation for PPTA

Vibrations with phase difference ϕ	Frequencies of LAM
4°	3.6
5°	4.6
10°	9.1

Given the satisfactory calculated results obtained, we have estimated the ultimate tensile modulus by two particular techniques. In the first estimate, we have taken only the diagonal force constants used in this analysis and obtained a value of 184 GPa using Treloar's method. However, a much more satisfactory analysis is available to us. We have calculated the dispersion curve associated with PPTA and obtained the modulus value by measuring the slope of the longitudinal vibrations near the zone centre, i.e. all the vibrations of translational repeat are moving in-phase. The modulus obtained by this technique is based on a well characterized structure and the complete set of force constants developed independently. We obtained a value of 241 GPa, which is much higher than previous calculations or experimental results. Finally, the spectroscopic analysis was also useful in following the water uptake by measuring the exchange between N–H and N–D of the amide groups. Details of this analysis will be published separately.

ACKNOWLEDGEMENTS

This research has been supported by the Petroleum Research Fund, grant number 14292-AC7. One of us (P.K.K.) is particularly appreciative of the partial fellowship support from the Santos Go award.

REFERENCES

1 Black, W. B. *Am. Rev. Mater. Sci.* 1980, **10**, 311, and references therein
2 Haraguchi, K., Kajiyama, T. and Takayanagi, M. *J. Appl. Polym. Sci.* 1979, **23**, 903
3 Haraguchi, K., Kajiyama, T. and Takayanagi, M. *J. Appl. Polym. Sci.* 1979, **23**, 915
4 Northolt, M. G. *Eur. Polym. J.* 1974, **10**, 799
5 Yabuki, K., Ho, H. and Ota, T. *Sen.-i Gakkaishi* 1975, **31**, T524
6 Dobb, M. G., Johnson, D. J. and Saville, B. P. *J. Polym. Sci.-Phys.* 1977, **15**, 2201
7 Li, L. S., Allard, L. F. and Bigelow, W. C. *J. Macromol. Sci.-Phys.* 1983, **B22**, 269
8 Panar, M., Avakian, P., Blume, R. C., Gardner, K. H., Gierke, T. D. and Yang, H. H. *J. Polym. Sci.-Phys.* 1983, **21**, 1955

9 Penn, L. and Milanovich, F. *Polymer* 1979, **20**, 31
10 Venkatesh, G. M., Shen, D. Y. and Hsu, S. L. *J. Polym. Sci., Polym. Phys. Edn.* 1981, **19**, 1475
11 Shen, D. Y., Venkatesh, G. M., Burchell, D. J., Shu, P. H. C. and Hsu, S. L. *J. Polym. Sci., Polym. Phys. Edn.* 1982, **20**, 509
12 Shen, D. Y. and Hsu, S. L. *Polymer* 1982, **23**, 969
13 Shen, D. Y., Molis, S. E. and Hsu, S. L. *Polym. Sci. Eng.* 1983, **23**, 543
14 Shablygin, M. V., Belousova, T. A., Nikitina, O. A., Bondareva, L. V., Bondarenko, O. A., Volkhina, A. V., Takarev, A. V. and Kudryavtsev, G. I. *Polym. Sci. U.S.S.R.* 1982, **24**, 1388
15 Zhurkov, S. N., Vettegren, V. I., Korsukov, V. E. and Novak, J. I. *Fracture* 1969, **2**, 545
16 Wool, R. P. and Boyd, R. H. *J. Appl. Phys.* 1980, **51**, 5116
17 Miyazawa, T. *J. Polym. Sci.* 1961, **55**, 215
18 Shimanouchi, T., Asahina, M. and Enomoto, S. *J. Polym. Sci.* 1962, **59**, 93
19 Sakurada, I., Ito, T. and Nakamae, K. *J. Polym. Sci. C.* 1966, **15**, 75
20 Kim, P., Hsu, S. L. and Ishida, H. *Macromolecules*, in press
21 Treloar, L. R. G. *Polymer* 1960, **1**, 290
22 Fielding-Russell, G. S. *Text. Res. J.* 1971, **41**, 861
23 Sugeta, H. and Miyazawa, T. *Polymer J.* 1970, **1**, 226
24 Tashiro, K., Kobayashi, M. and Tadokoro, H. *Macromolecules* 1977, **10**, 413
25 Pulay, P., Fogarasi, G. and Boggs, J. E. *J. Chem. Phys.* 1981, **74**, 3999
26 La Lau, C. and Snyder, R. G. *Spectrochim. Acta* 1971, **27A**, 2073
27 Dwivedi, A. and Krimm, S. *Macromolecules* 1982, **15**, 177
28 Schachtschneider, J. H. and Snyder, R. G. *Spectrochim. Acta* 1963, **19**, 117
29 Penn, L. and Larsen, F. *J. Appl. Polym. Sci.* 1979, **23**, 59
30 Tsubomura, H. *J. Chem. Phys.* 1956, **24**, 927
31 Nakanishi, M., Tsuboi, M., Ikegami, A. and Kanehisa, M. *J. Mol. Biol.* 1972, **64**, 363
32 Gaymans, R. J., Tijssen, J., Harkema, S. and Bantjes, A. *Polymer* 1976, **17**, 517